

Using the PhotoStress Method to Determine the Residual Stresses

HUSSEIN ALZYOD¹, PETER FICZERE²

¹Budapest University of Technology and Economics, Faculty of Transportation Engineering and Vehicle Engineering, Department of Railway Vehicles and Vehicle System Analysis, hussein.alzyod@edu.bme.hu

²Budapest University of Technology and Economics, Faculty of Transportation Engineering and Vehicle Engineering, Department of Railway Vehicles and Vehicle System Analysis, ficzere.peter@kjk.bme.hu.

Strains and stresses in loaded and photoelastically coated structural members can be determined using the PhotoStress method. The quantitative values of variations in the principal strains (stresses) and their directions could be employed to get the strain or stress components field on the entire coated surface. In the PhotoStress experiment, isochromatic fringes give qualitative and quantitative information. It provides a source of information on the directions and magnitudes of principal strain and principal normal stress on the surface of photoelastic coated parts. This article reviews the principle of using PhotoStress analysis to measure the residual stress and provides the boundary condition of using this method.

Keywords: PhotoStress method, Residual stress, Photoelastic coating, boundary conditions.

Introduction

Residual stress is the stress that remains in a body that is in equilibrium with its surroundings. It can have a major effect on a material's efficiency or component life. Useful residual stresses could also be intentionally created (Alzyod & Ficzere, 2021). Recent mathematical and computational methodologies can help identify the stresses related to a component in service. This is inadequate for providing an accurate component efficiency prediction. In point of fact, in a large number of cases where the abrupt failure occurred, it was linked to the presence of residual stresses, which, when combined with service stresses, resulted in a significant reduction in part lifespan. One of the industry concerns is gaining a thorough understanding of residual stress. External influences such as temperature variations, irregular mechanical deformation, or phase change cause materials to deform nonuniformly during the material production process, resulting in residual stress that remains in the component after thermo-mechanical processing. They have a direct effect on a produced part's effectiveness like distortion, crack propagation, corrosion, and fatigue. Corrosion and fatigue account for more than half of all mechanical failures (Findlay & Harrison, 2002).

The first residual stress measurements were made in the 1930s, and many techniques have since been devised (Withers & Bhadeshia, 2013). They can be categorized into two groups based on whether or not the sample will be damaged: Hole-drilling, sectioning, ring core, crack compliance, and layer removal are examples of mechanical release methods (Schajer, 2010), whereas X-ray diffraction, PhotoStress

method, magnetics, ultrasonic, and Raman techniques are examples of physical release methods (Ager & Drory, 1993; Allen et al., 2006; International et al., n.d.; Trebu et al., n.d.). Mechanical release techniques damage the component by separating or splitting it locally to relieve the remaining stress. Strain gauges, Moiré interferometry, laser speckle interferometry, holography, and Digital Image Correlation (DIC) (ASTM, 2008; Nelson, 2010) are used to make measurements. These procedures are well-developed, and the theory behind them is well-understood. Non-destructive approaches include several well-known but somewhat costly technologies. X-ray diffraction is a surface measuring technique that could only be employed in particular crystal structures and is sensitive to surface treatment. Magnetic testing approaches are based on the changing interaction between stress and the magnetic distribution in the process of ferromagnetic saturation that could only be used on magnetic properties.

Furthermore, ultrasonic inspection is straightforward in concept and suited for insight residual stress measurements (Shui & Wang, 2011). However, certain challenges remain, such as identifying sound velocity variations caused by components flaws or stress (Jiang et al., n.d.; Luo et al., 2011). Mechanical release techniques, while less desirable than non-destructive procedures due to the distortion they cause to samples, are frequently the favoured option due to their adaptability and dependability. This paper will discuss the investigation of residual stress using the PhotoStress method.

Using the PhotoStress method to measure residual stress

Photoelastic coatings are the cornerstone of a stress analysis approach that is better than any other for analyzing surface stresses. The technology was created in the fifties of the last century, mostly because of F. Zandman's contributions (BLUM, 1977), and was dubbed the 'Photo Stress' approach at the time. It has the benefit of providing both great information and exact data regarding stress levels on the surface of objects and machine components at the same time.

PhotoStress is a commonly used full-field method for reliably detecting surface strains to quantify the stresses in a part or structure during static or dynamic testing. The PhotoStress technique begins with the test item being coated with a specific strain-sensitive plastic coating. The coating is then illuminated with polarized light from a reflection polariscope when the component is subjected to test or service loads. When seen via the polariscope, the coating shows the strains in a brightly coloured, instructive pattern, revealing the general distribution of and pinpointing highly stressed locations. Quantitative stress evaluation may be accomplished rapidly and simply with an optical compensator connected to the polariscope. Photos or video capture can be used to keep information and records of the total strain distribution. Photostress has many advantages features like identifying important locations in real-time, emphasizing highly stressed and under-stressed areas, defining stress distribution at holes, notches, fillets, and other probable fracture points by accurately measuring maximum stresses, minimizing weight and increasing dependability by optimizing stress distribution in components and structures, at every location on the coated object, measure the principal stresses and directions, without recoating the item, test it frequently under varied load circumstances, measure stress in the lab or in the outdoors, without regard for dampness or time, determine assembly stresses and residual stresses and quantify them, and evaluate redistribution of stresses in the plastic region of deformation and identify yielding (Redner, 1980). PhotoStress has a proven track record of success in virtually every field of

manufacturing and construction that uses stress analysis, including automobiles, farming equipment, aeroplanes and aviation, construction works, engines, marine structures. In crystals, however, the index is determined by the direction of the vibration with regard to the index axis. When unstressed, certain materials, particularly plastics, react isotropically, but they become optically anisotropic when stressed. Similar to the resistance change in a strain gauge, the change in the index of refraction is a function of the resultant strain when a polarized beam transmits through a transparent plastic with a thickness of t . where, X and Y are the principal strain directions at the position of interest. As seen in figure 1, the light vector divides, and two polarized beams propagate in the X and Y planes. If the strain intensity in X and Y is ϵ_x and ϵ_y , respectively, and the speed of light vibrating in these directions is V_x and V_y , the time required to pass the plate for each of them is t/V , and the proportional retardation between these two beams is:

$$\delta = C \left(\frac{t}{V_x} - \frac{t}{V_y} \right) = t(n_x - n_y) \quad (1)$$

Where: $n = \text{index of refraction}$.

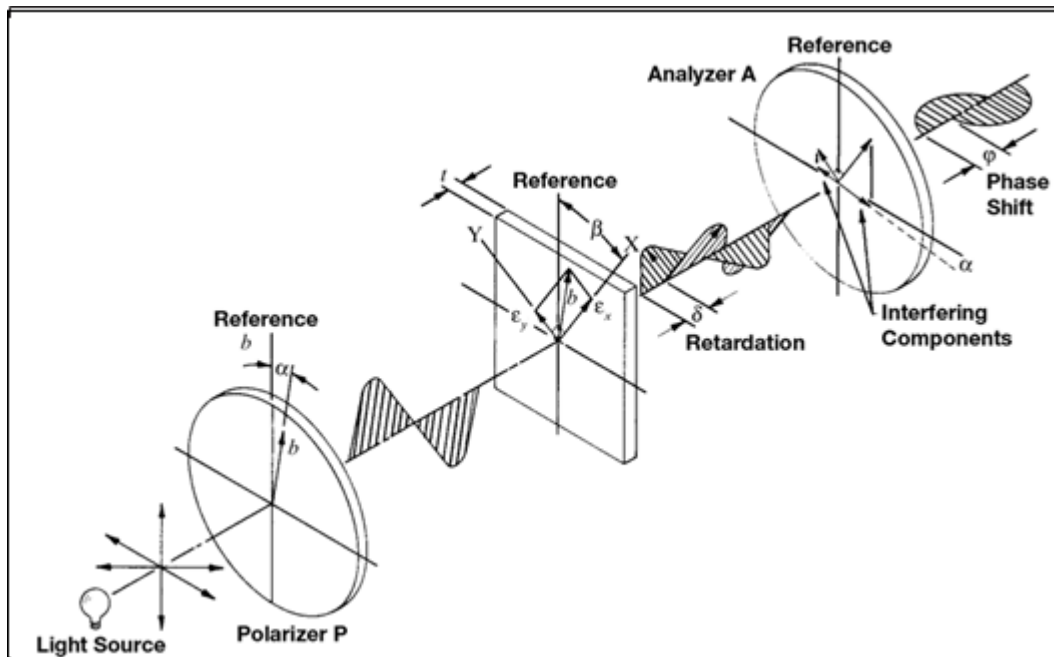


Figure 1. Plane polariscope [16].

Light travels at a speed of $3 \times 10^{10} \text{ cm/sec}$ in a vacuum or air. The speed V is lower in other transparent substances, and the ratio C/V is denoted the index of refraction. This index is constant in a homogeneous substance independent of propagation direction or vibration plane.

Brewster's law (stress optic law) states that: "The relative change in the index of refraction is proportional to the difference of principal strains" (Singh, 2015), or:

$$(n_x - n_y) = K(\epsilon_x - \epsilon_y) \quad (2)$$

The constant K is known as the "strain-optical coefficient," and it describes a material's physical attribute. It's a non - dimensional constant that's normally determined by calibration, and it's comparable to the "gage factor" of resistance strain gages. By combining the phrases mentioned above, we get:

$$\delta = tK(\varepsilon_x - \varepsilon_y) \quad \text{in transmission} \quad (3)$$

$$\delta = 2tK(\varepsilon_x - \varepsilon_y) \quad \text{in reflection (light passes through the plastic twice)} \quad (4)$$

As a result, the fundamental relationship for measuring strain with the PhotoStress (photoelastic coating) approach is:

$$(\varepsilon_x - \varepsilon_y) = \frac{\delta}{2tK} \quad (5)$$

When the two waves emerge from the plastic, they are no longer in phase because of the retardation. As shown in Figure 1, analyzer A will only transmit one element of these waves (parallel to A). The resultant light intensity will be a function of the retardation (δ) and the angle between the analyzer and the direction of the principal strains ($\beta - \alpha$). The intensity of light emerging from a plane polariscope will be:

$$I = b^2 \sin^2 2(\beta - \alpha) \sin^2 \frac{\pi\delta}{\lambda} \quad (6)$$

Where λ is the light wavelength.

When $\beta - \alpha = 0$, or when the crossed polarizer/analyzer is parallel to the direction of principal strains, the light intensity becomes zero. To measure the main strain directions, a plane polariscope configuration is employed.

When quarter-wave plates are placed in the path of light propagation, circularly polarized light is produced, as shown in figure 2, and the image perceived is unaffected by the direction of principal strains. As a result, the intensity of emerging light becomes:

$$I = b^2 \sin^2 \frac{\pi\delta}{\lambda} \quad (7)$$

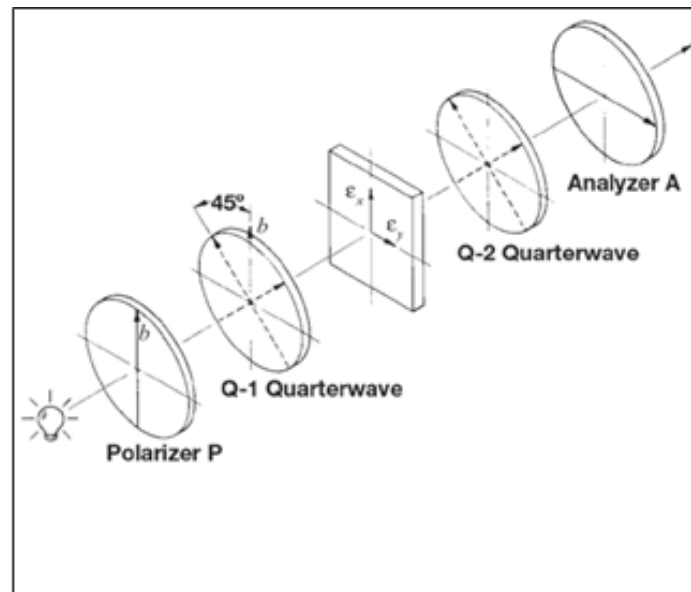


Figure 2. Circular polariscope(Introduction to Stress Analysis by the PhotoStress ® Method PhotoStress ® Instruments, 2011).

In a circular polariscope, the light intensity becomes zero when $\delta = N\lambda$ where N is 1,2,3,...etc. A reflection polariscope is used to monitor and measure the surface strains on the photoelastically coated test component for PhotoStress analysis. Figure 3 illustrates the schematic representation of the reflection polariscope (Adelfar et al., 2020).

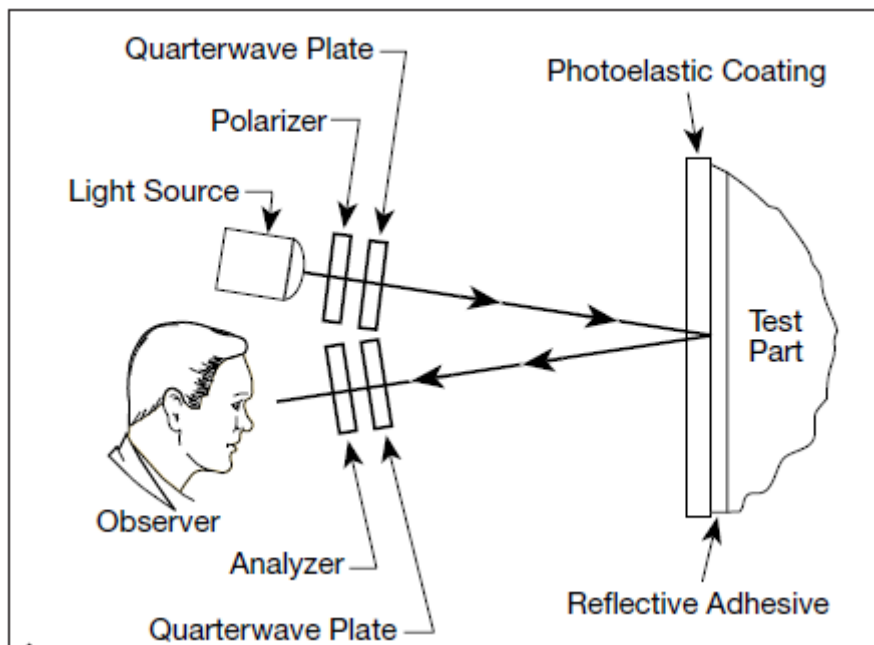


Figure 3. Schematic representation of reflection polariscope(Adelfar et al., 2020)

The number N is known as fringe order and illustrates the size of δ as shown in table 1(Frankovský et al., 2014). Once the $\delta = N\lambda$ is known, the principal strain difference is found by:

$$(\varepsilon_x - \varepsilon_y) = \frac{\delta}{2tK} = N \frac{\lambda}{2tK} = Nf \quad (8)$$

The fringe value (coating sensitivity), f , contains all constants, and N is the result of measurements.

Eq. (8) can be used to find the shear strain γ_{xy} :

$$\gamma_{xy} = Nf \quad (9)$$

Where: γ_{xy} = maximum shear strain (in the plane of the part surface at any point).

The relevance of the preceding is that by simply identifying the fringe order and multiplying by the fringe value of the coating, the variation in the principal strains, or the maximum shear strain on the surface of the test part, can be calculated.

Engineers and designers usually deal with stress rather than strain, and Eq. (8) and Eq. (9) can be translated for this purpose by applying Hooke's law to the biaxial stress state in mechanically isotropic materials:

$$\sigma_x = \frac{E}{1 - \nu^2} (\varepsilon_x + \nu\varepsilon_y) \quad (10)$$

$$\sigma_y = \frac{E}{1 - \nu^2} (\varepsilon_y + \nu\varepsilon_x) \quad (11)$$

$$\sigma_y = \frac{E}{1 + \nu} (\varepsilon_x - \varepsilon_y) \quad (12)$$

Substituting Eq. (8) into Eq. (12),

$$\sigma_x - \sigma_y = \frac{E}{1 + \nu} Nf \quad (13)$$

Where:

$\sigma_x - \sigma_y$ = principal stresses in test part surface

E = elastic modulus of the test part

ν = Poisson's ratio of the test part

Table 1. Isochromatic Fringe characteristics(Frankovský et al., 2014)

Colour	Approximate Relative Retardation (nm)	Fringe Order N
 Black	0	0.0
 Pale Yellow	345	0.60
 Dull red	520	0.90
 Red/Blue Transition	575	1.00
 Blue-Green	700	1.22
 Yellow	800	1.39
 Rose-red	1050	1.82
 Red/Green Transition	1150	2.00
 Green	1350	2.35
 Yellow	1440	2.50
 Red	1520	2.65
 Red/Green Transition	1730	3.00
 Green	1800	3.10

White light is made up of all wavelengths in the optical spectrum and is commonly utilized for full-field analysis of fringe patterns in PhotoStress analysis. As a result, the relative retardation that causes the extinction of one wavelength (colour) does not always induce the extinction of others. When every colour in the spectrum is extinguished in order of wavelength (beginning with violet, the shortest visible wavelength) with increasing birefringence, the observer sees the complementary colour that makes up the visible fringe pattern in white light. Fringe identification on a test sample exposed to uniaxial tension stress is shown in Figure 4 (*Introduction to Stress Analysis by the PhotoStress® Method PhotoStress® Instruments*, 2011). The higher-order fringes get fainter than the first due to the simultaneously repeated extinction of colours and lie in the transitional zone between red and green. In white light, fringe orders higher than 4 and/or 5 are not recognizable by colour.

Since higher-order fringes are hardly found (or required) in stress and strain analysis with PhotoStress coatings, extremely high-order fringes may always be identified with the Model 036 Monochromator and the reflection polariscope. Because the fringes never overlap or lose their identifiers, the fringe order and strain level are consistent throughout the fringe. Furthermore, the fringes are always in a continuous series in terms of quantity and colour. To put it in other words, if the first- and third-order fringes are known, the second-order fringe must be somewhere in the middle. The colour sequence

determines whether the fringe order and strain level rise or decline in each direction (Ficzere & Borbás, 2016).

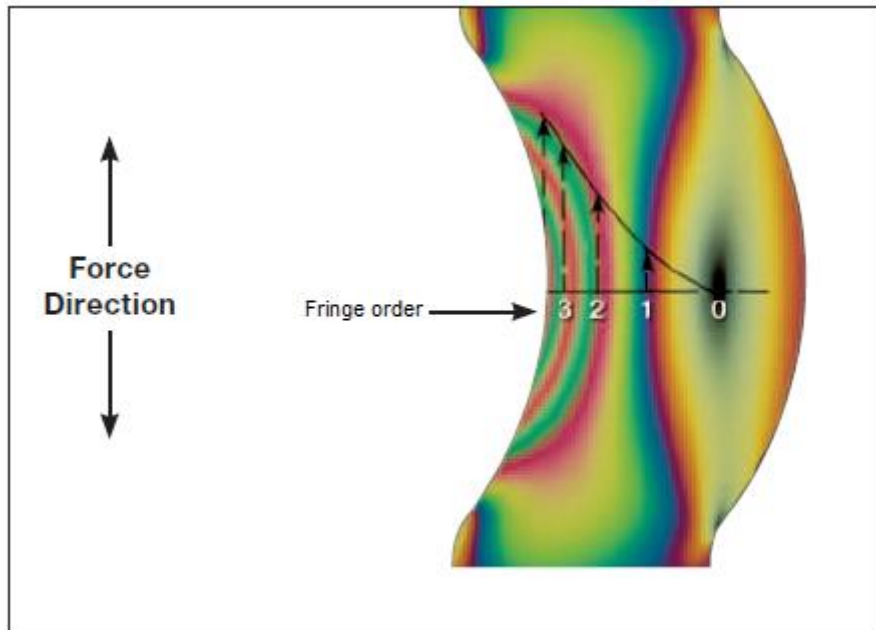


Figure 4. Strain field with fringes identified (Introduction to Stress Analysis by the PhotoStress® Method PhotoStress® Instruments, 2011).

Boundary conditions of using PhotoStress coatings

The choosing of materials of PhotoStress coating is just crucial to this form of empirical stress analysis like the choosing of gage and adhesive is to the strain gage method. Since choosing the materials of coating is mostly a question of reason and logic, it is beneficial to follow a step-by-step approach to avoid neglecting one or more crucial factors. The main goal is to find coating substances that would provide superior reliability and precision within particular test conditions, costing the least effort and expenditure. Because so many aspects influence a PhotoStress coating's performance, a compromise is sometimes required. The ideal strategy is to make a list of all the relevant aspects for the application and address the most significant needs first. The main factors in choosing a PhotoStress coating for certain test circumstances are the plastic application method to the test surface, sharpness of the contour, the effect of reinforcing, sensitivity, greatest elongation, and testing temperature.

1. Plastic application method to the test surface

There are two primary types of photoelastic coatings: sheets that are completely flat and casting fluids for contourable sheets (Borbás, 2000). Numerous materials of coating with different types are accessible. These materials may be categorized into three groups based on their elastic modulus: high-modulus materials, medium-modulus materials, and low-modulus materials. When the test component that is required to be coated has a flat surface, flat sheets are preferred because they offer many benefits such as uniform thickness (tolerance varies based on the material type), uniform physical and photoelastic characteristics, handling easily. In contrast, fluid plastic has to be chosen and applied with

the contoured-sheet approach for nonuniformly shaped components that could not be covered using flat sheets.

2. The sharpness of the contour

When sheets must be curved over extremely complicated surfaces, another situation when a thinner, less sensitive covering may be needed, suppose the coating surface has a curvature with a small radius. In that case, the coating thickness must be chosen to allow the sheets to be curved over the protrusion and into the recesses while maintaining an equal thickness. As a general rule, the sheet thickness must not exceed 10% of the surface's diameter. For simply curved surfaces, slightly larger thicknesses are acceptable.

3. Effect of reinforcing

A thick coating can have a considerable reinforcing impact in some circumstances, which must be taken into consideration if precise results are to be attained. The reinforcement generated by the plastic coating on structural components like "U," "H," "I," or rectangular cross-section beams, as well as thick wall parts, tube-shaped structure, and castings is insignificant and may be neglected. The reinforcing effect is generally unimportant for plane-stress issues and membrane stresses created under bending. Yet, if thin beams are twisted, the test component will be reinforced significantly by the plastic covering. So, to overcome the plastic covering impact, the measured strain should be corrected. In the case of low modulus substances, the effect of reinforcing for plane stress must not be omitted and should be adjusted. The variables that cause bending reinforcement error are: the unbiased plane moves closer to the coating, the coating strain is larger than the test specimen's surface, the section stiffens, and so the curve caused by a given bending moment is reduced, and the photoelastic measurement is averaged along with the plastic. It should be noted that the third and fourth variables mentioned above are photoelastic and geometric impacts, respectively, rather than reinforcing effects. However, as illustrated in Figure 5, all four effects work together, making it easier to combine the errors and fix the data with a single correction factor.

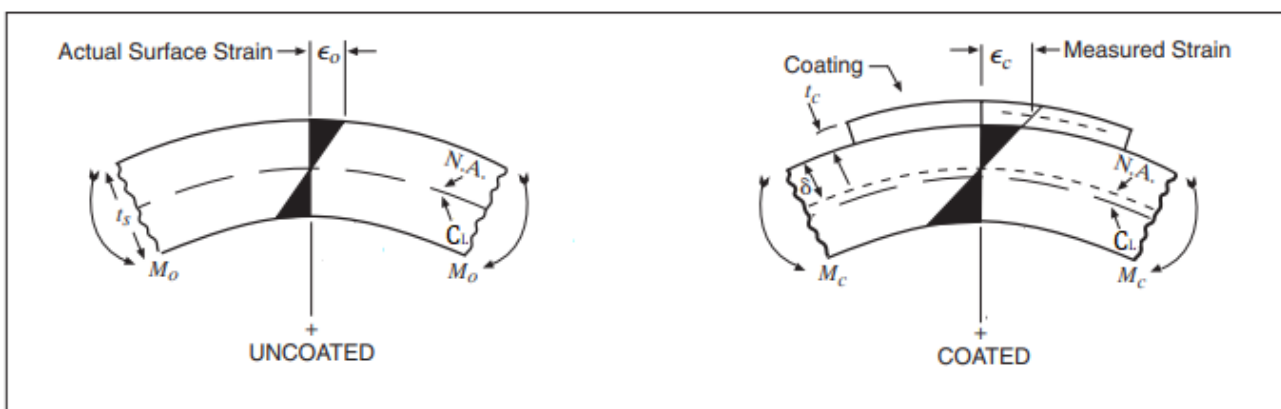


Figure 5. Schematic showing bending reinforcement

4. Sensitivity

Because this feature is included in the fundamental equation (Eq. 8), the birefringent sensitivity of the plastic material may be the single most significant factor to consider when selecting a photoelastic coating. Two factors mainly determine the total sensitivity of strain measurement:

1. The coating's sensitivity, as measured by the fringe value, The difference in primary strains, or the highest shear strain, necessary to generate one fringe is represented by the fringe value. The coating becomes more sensitive as this value decreases.
2. The polariscope system's sensitivity to inspect the photoelastic pattern and detect the fringe order, N.

The number of fringes that should be seen can be determined before experimenting. For manual analysis, a range of one to four is typical. When the predicted level of the strain can be determined, the required number of coating sensitivity or fringe may be computed from Eq. (8) as follows:

$$f = \frac{(\varepsilon_x - \varepsilon_y)}{N} = \frac{(\text{anticipated strain})}{(\text{desired } N_{max})} \quad (14)$$

The predicted strain level would match the material's incipient yielding in an ideal world. However, prescribed test and loading circumstances frequently impose a lower strain level. When the fringe value obtained by using the estimated strain level and the number of fringes, the following expression may be used to find the type and thickness of plastic that will fulfil the sensitivity demand.

$$f = \frac{\lambda}{2tK} \quad (15)$$

This relation has been represented in figure 6 (*How to Select Photoelastic Coatings PhotoStress® Instruments*, 2015) for clarity of plastic choosing. Figure 6 represents the thickness of the coating and the bands of the strain-optic factor for which materials are easily accessible. To utilize the chart, input the proper value off along the ordinate and go into the horizontal direction until you find a crossing with a diagonal thickness line that lies inside one of the shaded regions. This crossing determines a K-value from the horizontal axis and a coating thickness that meets the sensitivity criteria. In case of no intersection can be located, working with lower sensitivity and fewer fringes will be essential.

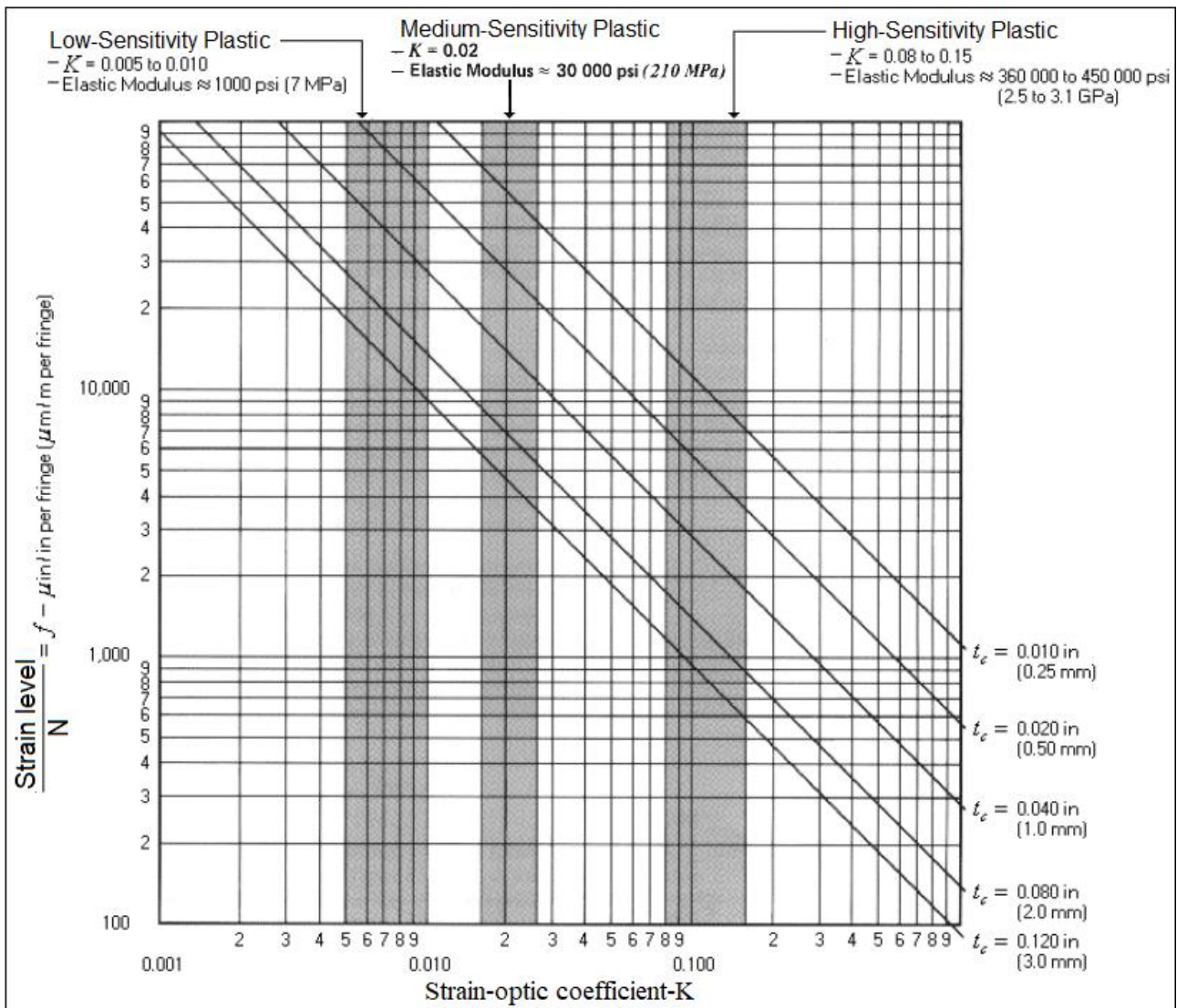


Figure 6. Relation between coating thickness, fringe constant, and Strain-optic coefficient (How to Select Photoelastic Coatings PhotoStress © Instruments, 2015).

5. Greatest elongation

The highest measured strain for a given coating of photoelastic is determined by the stress-strain curve and photoelastic behaviour's linearity. The allowed elongations for various common coatings are shown in Table 2. The coating performance determining totally plastic stresses in metallic elements differs from that needed for measuring elastoplastic strains. Because of the large strains contained in plastic strains, coating sensitivity is less important. The coating capability to track the metal into the plastic zone is the most important aspect. This problem can be resolved by applying a very thin plastic coating with a high modulus of elasticity or by applying a thick plastic coating with a low modulus of elasticity.

Table 2. Allowable elongations for some typical coatings (Ingle et al., 2016).

Type of coating Material	Maximum Elongation (%)	Application
PS-1	5	In the elastic and elastoplastic ranges, testing on metals, concrete, glass, and hard plastics.
PS-10	3	
PL-1	3	
PL-10	3	
PS-3	30	Soft materials, such as rubber, plastics, and wood, are subjected to testing.
PL-2	50	
PL-3	>50	
PS-4	>40	
PS-6	>100	Rubber, plastics, and wood are among the soft materials tested.

6. Testing temperature.

If the measurement is to be conducted at a temperature different from ambient temperature, the impact of temperature on the coating's behaviour must be considered. The technical information on the coating label relates to the material's room temperature characteristics. Several of these parameters will be changed if the temperature changes throughout the test. Consider, for instance, the strain-optic factor, K . The general way the strain-optic coefficient changes with temperature for standard coating materials is shown in Figure 7 (Ingle et al., 2016). The coatings (except PS-1) usually have two temperature ranges that quickly change. While the plastics can be employed in either constant- K or variable- K ranges, it is essential to choose a material with constant K across the temperature range of the test. F. Zandman, S. Redner, and D. Post. (Zandman et al., n.d.) proposed a detailed analysis for additional thermal effects that should be considered.

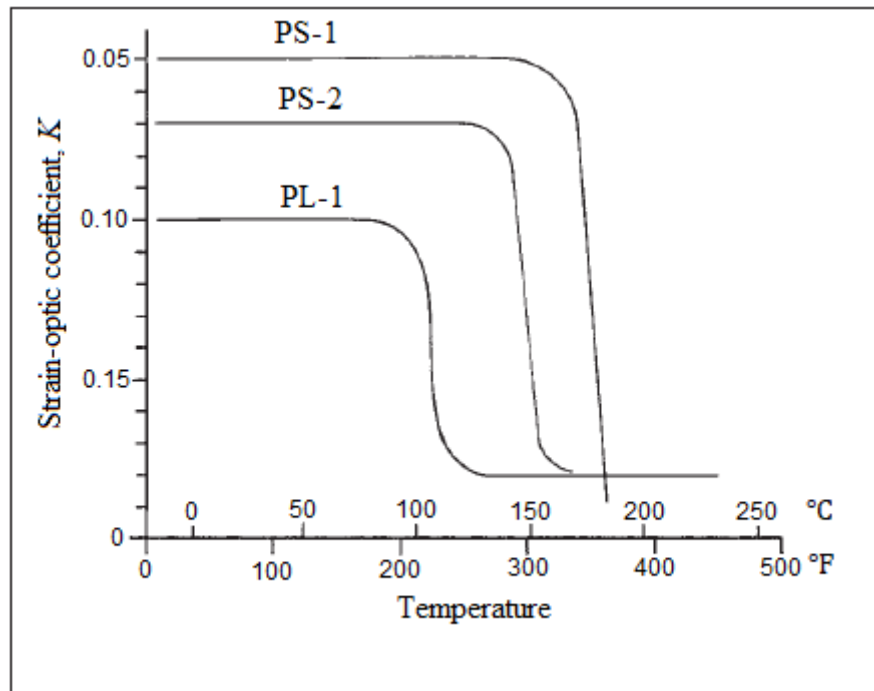


Figure 7. Strain-optic coefficient Vs. Temperature for typical coating materials (Ingle et al., 2016).

Conclusion

Photoelastic coatings are the core of a stress analysis method that is superior to all others in terms of assessing surface stresses. Some parameters should be considered while using the PhotoStress technique like plastic application method to the test surface, sharpness of the contour, the effect of reinforcing, sensitivity, greatest elongation, and testing temperature.

References

- [1] Adelfar, M., Tavangar, R., Horandghadim, N., & Khalil-Allafi, J. (2020). Evaluating superelastic and shape memory effects using the photostress technique. *Materials Today Communications*, 24, 101156. <https://doi.org/10.1016/J.MTCOMM.2020.101156>
- [2] Ager, J. W., & Drory, M. D. (1993). Quantitative measurement of residual biaxial stress by Raman spectroscopy in diamond grown on a Ti alloy by chemical vapor deposition. *Physical Review B*, 48(4), 2601–2607. <https://doi.org/10.1103/PHYSREVB.48.2601>
- [3] Allen, A. J., Hutchings, M. T., Windsor, C. G., & Andreani, C. (2006). Neutron diffraction methods for the study of residual stress fields. *Http://Dx.Doi.Org/10.1080/00018738500101791*, 34(4), 445–473. <https://doi.org/10.1080/00018738500101791>

- [4] Alzyod, H., & Ficzer, P. (2021). RESIDUAL STRESSES IN ADDITIVE MANUFACTURING. *GÉP LXXII*, 3–4, 41–44.
- [5] ASTM. (2008). *ASTM E837-08: Standard Test Method for Determining Residual Stresses by the Hole-Drilling Strain-Gage Method*.
- [6] BLUM, A. E. (1977). The use and understanding of photoelastic coatings. *Strain*, 13(3), 96–101. <https://doi.org/10.1111/J.1475-1305.1977.TB00238.X>
- [7] Borbás, L. (2000). Investigation of structural components by photoelastic coating technique. In *Engineering Design and Industrial Design Interaction* (pp. 18–37). Bologna University International Centre–Bertinoro (Forli) Italy.
- [8] Ficzer, P., & Borbás, L. (2016). New Application of 3D Printing Method for Photostress Investigation. *Materials Today: Proceedings*, 3(4), 969–972. <https://doi.org/10.1016/J.MATPR.2016.03.030>
- [9] Findlay, S. J., & Harrison, N. D. (2002). Why aircraft fail. *Materials Today*, 5(11), 18–25.
- [10] Frankovský, P., Trebuňa, F., Kostka, J., Šimčák, F., Ostertag, O., & Papacz, W. (2014). Characteristic Entities in PhotoStress Method. *American Journal of Mechanical Engineering*, 2(7), 239–243. <https://doi.org/10.12691/ajme-2-7-13>
- [11] *How to Select Photoelastic Coatings PhotoStress® Instruments*. (2015). www.micro-measurements.com
- [12] Ingle, A. H., Vanalkar, A. v., & Khandare, S. S. (2016). Photo Elastic Coating Materials in Thermo-Photo Elasticity. *Research Inventy: International Journal of Engineering And Science*, 6(5), 33–47. www.researchinventy.com
- [13] International, P. P.-A., Handbook., A., & 1986, undefined. (n.d.). X-ray diffraction residual stress techniques. *Shotpeener.Com*. Retrieved January 9, 2022, from <https://www.shotpeener.com/library/pdf/1986155.pdf>
- [14] *Introduction to Stress Analysis by the PhotoStress® Method PhotoStress® Instruments*. (2011). www.vishaymg.com
- [15] Jiang, G., Tan, M., Wang, W., hydraulics, W. H.-M. tool &, & 2007, undefined. (n.d.). Present research status of measuring residual stress. *En.Cnki.Com.Cn*. Retrieved January 9, 2022, from https://en.cnki.com.cn/Article_en/CJFDTotat-JCYY200706073.htm
- [16] Luo, Y., Wang, Z., Xu, B., & Yuan, F. (2011). The pre-stack migration imaging technique for damages identification in concrete structures. *Theoretical and Applied Mechanics Letters*, 1(5), 051004. <https://doi.org/10.1063/2.1105104>
- [17] Nelson, D. v. (2010). Residual stress determination by Hole drilling combined with optical methods. *Experimental Mechanics*, 50(2), 145–158. <https://doi.org/10.1007/S11340-009-9329-3/FIGURES/19>
- [18] Redner, A. S. (1980). Photoelastic coatings. *Experimental Mechanics 1980 20:11, 20(11)*, 403–408. <https://doi.org/10.1007/BF02321016>

- [19] Schajer, G. S. (2010). Relaxation Methods for Measuring Residual Stresses: Techniques and Opportunities. *Experimental Mechanics*, 50(8), 1117–1127. <https://doi.org/10.1007/S11340-010-9386-7/FIGURES/8>
- [20] Shui, G., & Wang, Y. (2011). Characterization of surface damage of a solid plate under tensile loading using nonlinear Rayleigh waves. *Theoretical and Applied Mechanics Letters*, 1(5), 051005. <https://doi.org/10.1063/2.1105105>
- [21] Singh, Devraj. (2015). *Fundamentals of optics*.
- [22] Trebu, F., Frankovsk, P., & Jadlovska, J. (n.d.). *NEW APPROACHES TO ASSESSMENT OF STRESS AND STRAIN FIELDS WITH APPLICATION OF PHOTOSTRESS METHOD*.
- [23] Withers, P. J., & Bhadeshia, H. K. D. H. (2013). Residual stress. Part 1 – Measurement techniques. <Http://Dx.Doi.Org/10.1179/026708301101509980>, 17(4), 355–365. <https://doi.org/10.1179/026708301101509980>
- [24] Zandman, F., Redner, S. S., & Post, D. (n.d.). *Photoelastic-coating Analysis in Thermal Fields*.